

# A New Hydrodynamic Model for Numerical Simulation of Interacting Galaxies on Intel Xeon Phi Supercomputers

Igor Kulikov<sup>1</sup>, Igor Chernykh<sup>1</sup>, and Alexander Tutukov<sup>2</sup>

<sup>1</sup> Institute of Computational Mathematics and Mathematical Geophysics SB RAS, 6-th Lavrentyev avenue, Novosibirsk, Russian Federation

<sup>2</sup> Institute of Astronomy RAS, 48-th Pyatnitskaya Street, Moscow, Russian Federation

E-mail: kulikov@ssd.ssc.ru

**Abstract.** This paper presents a new hydrodynamic model of interacting galaxies based on the joint solution of multicomponent hydrodynamic equations, first moments of the collisionless Boltzmann equation and the Poisson equation for gravity. Using this model, it is possible to formulate a unified numerical method for solving hyperbolic equations. This numerical method has been implemented for hybrid supercomputers with Intel Xeon Phi accelerators. The collision of spiral and disk galaxies considering the star formation process, supernova feedback and molecular hydrogen formation is shown as a simulation result.

## Introduction

The collisions between galaxies as they move in dense clusters is an important evolutionary factor because an ordinary galaxy can experience up to ten collisions with other galaxies in the Hubble time [1]. Observational and theoretical investigation of interacting galaxies is an indispensable method for studying their properties and evolution. The processes of star formation [2], AGN [3], the formation of supermassive binary black holes [4, 5], and chemodynamics [6] significantly accelerate the collision of galaxies. On the subject of research on collision of galaxies, it is worth mentioning the GALMER project of the Parisian observatory. This project consists of a database of computing experiments [7] on collisions of various types of galaxies.

The collisionless components of galaxies are usually described by means of the N-body model. This model is standard for this problem but also has some disadvantages. From the perspective of subgrid physical processes, the N-body model does not allow the total energy of a system to be maintained. As with the star formation processes (or explosion of supernova stars), we can keep only the mass of the system and the moment of an impulse. However, in this case, the thermodynamic coherence of the system is lost. That is, in the case of phase transition from gas, it is impossible to transform internal energy to particles. From the perspective of a numerical method, it is rather difficult to coordinate methods for the solution of hydrodynamic equations and particle dynamics. This is connected with the need to provide a sufficient number of particles in the case of a combination with mesh-based methods. The problem is partially solved by SPH methods, but they have shortcomings that will be described further. In the case of PIC methods, parallel realizations require many difficult algorithms of load balancing.



Advantages of SPH:	Advantages of AMR:
Robustness of algorithm	Approved methodology
Galilean invariant	Lack of artificial viscosity
Simplicity of realization	Correctness on a shock wave
Adaptation for geometry of a problem	Turbulence Reproduction
High precision of gravity	Reproduction of instability
SPH disadvantages:	AMR disadvantages:
Artificial viscosity	Complexity of realization
Radius of smoothing	Mesh effects
Oscillation on shock waves	Problem of mesh resolution
Suppression of instability	Problem of invariancy
Weak scalability	Weak scalability

**Table 1.** Advantages and disadvantages of SPH and AMR methods

As an alternative to the N-body model, there is a model based on the first moments of the Boltzmann equation [8]. The possibility of using this model for the description of the collisionless components of colliding galaxies [9] was experimentally proved. Sufficient conditions for the Boltzmann equation model are clustering star components, prevailing kinetics of the system and a lack of heat transfer effects.

In the last two decades, from the wide range of hydrodynamic numerical methods for the solution of nonstationary three-dimensional astrophysical problems, two main approaches have been used: the Lagrangian approach, which is generally presented by the SPH method (Smoothed Particle Hydrodynamics), and the Euler approach, which uses adaptive grids or AMR (Adaptive Mesh Refinement). In the last five years, several codes have been developed as combinations of Lagrangian and Euler approaches. The Lagrangian approach (SPH method) is used in Hydra [10], Gasoline [11], GrapeSPH [12], GADGET [13] packages. The Eulerian approach (including AMR) is used in NIRVANA [14], FLASH [15], ZEUS [16], ENZO [17], RAMSES [18], ART [19], Athena [20], Pencil Code [21], Heracles [22], Orion [23], Pluto [24], CASTRO [25] codes. The Eulerian approach with AMR was first used on hybrid supercomputers equipped with graphic accelerators in a GAMER code [26]. The advantages and disadvantages of these methods are given in table 1. BETHE-Hydro [27], AREPO [28], CHIMERA [29], GIZMO [30], and author's PEGAS/GPUPEGAS/AstroPhi [9, 31, 32] codes are based on Lagrangian and Eulerian approaches. This combination of methods solves the main problems of the approaches as described above.

In the first section, we will describe the mathematical model of the interacting galaxies. We will describe a numerical method of the solution and parallel realization in the second section. In chapter 3, the results of the computational experiment of spiral and disk galaxy collision will be shown.

## 1. Mathematical model

To account for chemical reactions, we will consider the equations of multicomponent single-speed gas dynamics. For the description of collisionless components, we will use the equations for the first moments of the collisionless Boltzmann equation. Our model includes star formation processes, supernova feedback, formation of molecular hydrogen and the cooling/heating function.

To describe the gas components, we will use the system of single-speed component

gravitational hydrodynamics equations, which is written in Euler coordinates:

$$\begin{aligned}\frac{\partial \rho}{\partial t} + \nabla \cdot (\rho \vec{u}) &= \mathcal{S} - \mathcal{D}, & \frac{\partial \rho \vec{u}}{\partial t} + \nabla \cdot (\rho \vec{u} \vec{u}) &= -\nabla p - \rho \nabla(\Phi) + \vec{v} \mathcal{S} - \vec{u} \mathcal{D}, \\ \frac{\partial \rho_H}{\partial t} + \nabla \cdot (\rho_H \vec{u}) &= -s_{H,H_2} + \mathcal{S} \frac{\rho_H}{\rho} - \mathcal{D} \frac{\rho_H}{\rho}, & \frac{\partial \rho_{H_2}}{\partial t} + \nabla \cdot (\rho_{H_2} \vec{u}) &= s_{H,H_2} + \mathcal{S} \frac{\rho_{H_2}}{\rho} - \mathcal{D} \frac{\rho_{H_2}}{\rho}, \\ \frac{\partial \rho E}{\partial t} + \nabla \cdot (\rho E \vec{u}) &= -\nabla \cdot (p \vec{v}) - (\rho \nabla(\Phi), \vec{u}) - \Lambda + \Gamma + \varepsilon \frac{\mathcal{S}}{\rho} - \varepsilon \frac{\mathcal{D}}{\rho}, \\ \frac{\partial \rho \varepsilon}{\partial t} + \nabla \cdot (\rho \varepsilon \vec{u}) &= -(\gamma - 1) \rho \varepsilon \nabla \cdot \vec{u} - \Lambda + \Gamma + \varepsilon \frac{\mathcal{S}}{\rho} - \varepsilon \frac{\mathcal{D}}{\rho}, & \rho E &= \frac{1}{2} \rho \vec{u}^2 + \rho \varepsilon, & p &= (\gamma - 1) \rho \varepsilon.\end{aligned}$$

To describe the collisionless components, we will use the system of equations for the first moments of the Boltzmann collisionless equation, which is also written in Eulerian coordinates:

$$\begin{aligned}\frac{\partial n}{\partial t} + \nabla \cdot (n \vec{v}) &= \mathcal{D} - \mathcal{S}, & \frac{\partial n \vec{v}}{\partial t} + \nabla \cdot (n \vec{v} \vec{v}) &= -\nabla \Pi - n \nabla(\Phi) + \vec{u} \mathcal{D} - \vec{v} \mathcal{S}, \\ \frac{\partial \rho W}{\partial t} + \nabla \cdot (\rho W \vec{v}) &= -\nabla \cdot (\Pi \vec{v}) - (n \nabla(\Phi), \vec{v}) + \varepsilon \frac{\mathcal{D}}{\rho} - \varepsilon \frac{\mathcal{S}}{\rho}, \\ \frac{\partial \Pi_{\xi\xi}}{\partial t} + \nabla \cdot (\Pi_{\xi\xi} \vec{v}) &= -2\Pi \nabla \cdot \vec{u} + \varepsilon \frac{\mathcal{D}}{3\rho} - \varepsilon \frac{\mathcal{S}}{3\rho}, & \rho W &= \frac{1}{2} \rho \vec{v}^2 + \frac{\Pi_{xx} + \Pi_{yy} + \Pi_{zz}}{2}.\end{aligned}$$

The Poisson equation can be written as:

$$\Delta \Phi = 4\pi G(\rho + n),$$

where  $p$  – gas pressure,  $\rho_H$  – density of atomic hydrogen,  $\rho_{H_2}$  – density of molecular hydrogen,  $s_{H,H_2}$  – speed of formation of molecular hydrogen from atomic,  $\rho = \rho_H + \rho_{H_2}$  – density of gas mixture,  $n$  – density collisionless component,  $\vec{u}$  – speed gas component,  $\vec{v}$  – speed collisionless component,  $\rho E$  – density of total mechanical gas energy,  $\rho W$  – density of total mechanical collisionless components energy,  $\Phi$  – gravitational potential,  $\varepsilon$  – density of internal energy of gas,  $\gamma$  – adiabatic index,  $\Pi_{\xi\xi} = (\Pi_{xx}, \Pi_{yy}, \Pi_{zz})$  – a diagonal tensor of dispersion of speeds collisionless components,  $\mathcal{S}$  – the speed of formation of supernova stars,  $\mathcal{D}$  – star formation speed,  $\Lambda$  – function of Compton cooling,  $\Gamma$  – function of heating from explosion of supernova stars.

Hydrogen molecules in intergalactic space are formed on a surface of particles and dissociated space radiation. Assuming that the density of gas is proportional to the density of particle concentration of molecular hydrogen [33] because of the good mixing of particles and gas in our model, it can be written as:

$$\frac{dn_{H_2}}{dt} = R_{gr}(T) n_H (n_H + 2n_{H_2}) - (\xi_H + \xi_{diss}(N_{H_2}, A_V)) n_{H_2},$$

where  $n_{H_2}$  and  $n_H$  – concentration of molecular and atomic hydrogen,  $N_{H_2}$  – the column density of molecular hydrogen, speed of formation of molecular hydrogen on dust is set by function [34] of  $R_{gr}(T) = 2.2 \times 10^{-18} S \sqrt{T} \text{ s}^{-1}$ , where  $S = 0.3$  – efficiency of formation of molecular hydrogen on dust [35], speed of ionization of hydrogen by the space beams is set by function [36, 37]  $\xi_H = 6 \times 10^{-18} \text{ s}^{-1}$ , where  $A_V$  – extinction [38]. Photodissociation rate in the form of [39]  $\xi_{diss}(N_{H_2}, A_V) = \xi_{diss}(0) f_{shield}(N_{H_2}) f_{dust}(A_V)$ , where  $\xi_{diss}(0) = 3.3 \times 1.7 \times 10^{-11} \text{ s}^{-1}$  – unshielded photodissociation rate [40],  $f_{dust}(A_V) = \exp(-\tau_{d,1000}(A_V))$  – absorption rate on dust [39], where  $\tau_{d,1000}(A_V) = 3.74 A_V = 10^{-21} (N_H + N_{H_2})$  – optical depth on dust particles on

wavelength  $\lambda = \text{\AA}1000$ , where  $N_H$  and  $N_{H_2}$  – column density. The function of the coefficient of self-shielding can be approximated [39]:

$$f_{shield}(N_{H_2}) = \frac{0.965}{(1 + x/b_5)^2} + \frac{0.035}{\sqrt{1+x}} \exp\left(-8.5 \times 10^{-4} \sqrt{1+x}\right),$$

where  $x = N_{H_2}/5 \times 10^{10} \text{ m}^2$ ,  $b_5 = b/10^7 \text{ m/s}$ , where  $b$  – the parameter of Doppler expansion. After calculation of molecular hydrogen concentration  $n_{H_2}$ , the adiabatic index [41] is defined:

$$\gamma = \frac{5n_H + 7n_{H_2}}{3n_H + 5n_{H_2}}$$

The equation for the description of hydrogen concentration dynamics has the analytical solution which was used in realization.

We will use the following necessary condition of process of star formation formulated in the form of [42]:

$$T < 10^4 K \quad \nabla \cdot \vec{u} < 0 \quad \rho > 1.64 \frac{M_\odot}{pc^{-3}}$$

The speed of star formation can be formulated as  $\mathcal{D} = \mathcal{C} \rho^{3/2} \sqrt{\frac{32G}{3\pi}}$ , where  $\mathcal{C} = 0.034$  – star formation efficiency. Speed of supernova stars formation [43] can be written as  $\mathcal{S} = \beta \mathcal{C} n^3 / 2 \sqrt{\frac{32G}{3\pi}}$ , where  $\beta = 0.1$  – coefficient of young stars explosion. The explosion energy of one solar mass star emitted is  $10^{51} \text{ erg}$ . In this case the heat function can be written as  $\Gamma = 10^{51} \frac{M^{SN}}{M_\odot} \text{ erg}$ , where  $M^{SN}$  – the mass of supernova stars in local volume.

The galactic gas which is warmed by collisions to temperature  $\sim 10^4 - 10^8 \text{ K}$  is described by the cooling function [44]  $\Lambda \simeq 10^{-22} n_H^2 \text{ cm}^{-3} \text{ erg}$ , where  $n_H$  – concentration of atomic hydrogen.

## 2. Numerical method

To solve the hydrodynamic equations, the original numerical method based on a combination of the operator splitting approach, Godunov's method, the Roe scheme and piecewise-parabolic reconstruction on a local stencil [45, 46] was used. This method unites all advantages of these methods and can be highly parallelized. To solve the Poisson equation, the FFT method is used.

At the Eulerian stage of a numerical method, the equations without the advective members and subgrid functions are solved. To approximate the spatial derivatives, the solution to a problem of the linearized Riemann's problem is used. For this purpose, the average speed and pressure (L – left cell, R – right cell) is calculated as follows:

$$\rho = \frac{\rho_L^{3/2} + \rho_R^{3/2}}{\sqrt{\rho_L} + \sqrt{\rho_R}}, \quad p = \frac{p_L \sqrt{\rho_L} + p_R \sqrt{\rho_R}}{\sqrt{\rho_L} + \sqrt{\rho_R}}.$$

This method of averaging is associated with accurate computation of the gas vacuum border. This averaging is more accurate than the original Roe scheme [47]. We will assume that the solution is a piecewise parabolic function in the considered cells. The detailed procedure of local parabola creation can be found in classical literature [48]. This procedure also must be used in the subsequent stage (the solution of Riemann's problem) of the method.

The solution of Riemann's problem (a detailed description of Godunov's scheme can be found in [49]) for the Eulerian stage can be written as:

$$U = \frac{u_L(-\lambda t) + u_R(\lambda t)}{2} + \frac{p_L(-\lambda t) - p_R(\lambda t)}{2} \sqrt{\frac{(\sqrt{\rho_L} + \sqrt{\rho_R})^2}{\frac{\gamma_L + \gamma_R}{2} (\rho_L^{3/2} + \rho_R^{3/2}) (p_L \sqrt{\rho_L} + p_R \sqrt{\rho_R})}},$$

$$P = \frac{p_L(-\lambda t) + p_R(\lambda t)}{2} + \frac{u_L(-\lambda t) - u_R(\lambda t)}{2} \sqrt{\frac{\frac{\gamma_L + \gamma_R}{2}(\rho_L^{3/2} + \rho_R^{3/2})(p_L \sqrt{\rho_L} + p_R \sqrt{\rho_R})}{(\sqrt{\rho_L} + \sqrt{\rho_R})^2}},$$

for collisionless component:

$$V = \frac{v_L(-\mu t) + v_R(\mu t)}{2} + \frac{\Pi_L(-\mu t) - \Pi_R(\mu t)}{2} \sqrt{\frac{(\sqrt{n_L} + \sqrt{n_R})^2}{3(n_L^{3/2} + n_R^{3/2})(\Pi_L \sqrt{n_L} + \Pi_R \sqrt{n_R})}},$$

$$\Pi = \frac{\Pi_L(-\mu t) + \Pi_R(\mu t)}{2} + \frac{v_L(-\mu t) - v_R(\mu t)}{2} \sqrt{\frac{3(n_L^{3/2} + n_R^{3/2})(\Pi_L \sqrt{n_L} + \Pi_R \sqrt{n_R})}{(\sqrt{n_L} + \sqrt{n_R})^2}}$$

where

$$\lambda = \sqrt{\frac{\frac{\gamma_L + \gamma_R}{2}(p_L \sqrt{\rho_L} + p_R \sqrt{\rho_R})}{\rho_L^{3/2} + \rho_R^{3/2}}}, \quad \mu = \sqrt{\frac{3(\Pi_L \sqrt{n_L} + \Pi_R \sqrt{n_R})}{n_L^{3/2} + n_R^{3/2}}},$$

$$q_L(-\nu t) = q_i^R - \frac{\nu t}{2h} \left( \Delta q_i - q_i^6 \left( 1 - \frac{2\nu t}{3h} \right) \right), \quad q_R(\nu t) = q_i^L + \frac{\nu t}{2h} \left( \Delta q_i + q_i^6 \left( 1 - \frac{2\nu t}{3h} \right) \right).$$

At the Lagrangian stage there is an advective transfer of hydrodynamic parameters and all equations can be written as:

$$\frac{\partial f}{\partial t} + \nabla \cdot (f \vec{v}) = 0,$$

where  $f$  can be density  $\rho$ ,  $n$ , can be impulse  $\rho \vec{u}$ ,  $n \vec{v}$ , total mechanically density  $\rho E$ ,  $nW$  or internal  $\rho \epsilon$ ,  $\Pi_{\xi\xi}$  energy of gas. A similar approach is used for the equations. This equation:

$$F = v \times \begin{cases} f_L(-\lambda t), v \geq 0 \\ f_R(\lambda t), v < 0 \end{cases},$$

is used for flux computation  $F = f \vec{v}$  with  $\lambda = |\vec{v}|$ . where  $f_L(-\lambda t)$   $f_R(\lambda t)$  – piecewise-parabolic function for  $f$ . The velocity on the interface between cells is calculated by:

$$v = \frac{v_L \sqrt{\rho_L} + v_R \sqrt{\rho_R}}{\sqrt{\rho_L} + \sqrt{\rho_R}}.$$

To create the piecewise and parabolic solution, the same procedure as in the previous stage is used. At the final stage of the hydrodynamic equations, a solution adjustment procedure is provided. In the case of a gas vacuum border, we use the procedure from [50]:

$$|\vec{v}| = \sqrt{2(E - \epsilon)}, (E - \vec{v}^2/2)/E \geq 10^{-3},$$

In the other area, an adjustment is used to guarantee non-decreasing entropy [51]:

$$|\rho \epsilon| = \left( \rho E - \frac{\rho \vec{v}^2}{2} \right), (E - \vec{v}^2/2)/E < 10^{-3},$$

This modification provides a detailed balance of energy and guarantees non-decreasing entropy.

The numerical method was verified on many problems: 1D problems of shock tube simulation, Kelvin–Helmholtz and Releigh–Taylor instabilities, Sedov blast wave problem, expansion of gas into a vacuum, Evrard’s collapse and other problems. Details of the tests can be found in [9, 31, 32, 49].

A geometrical decomposition of the computational area is based on the idea of parallel realization. The uniform numerical method allows the use of the identical geometrical decomposition scheme, which facilitates simpler and effective realization. Supercomputers with the RSC PetaStream-based architecture have been used for performance and scalability tests: MVS-10P (64x Intel Xeon Phi 7120D accelerators, each of which has 16 GB of integrated RAM, JSCC RAS). We use a grid size of 5123 on each accelerator for the MVS-10P tests. In our tests, we cannot use larger grid sizes for simulation of full numerical models. Computational experiments were performed at the RSC PetaStream architecture cluster of JSCC RAS with 134x acceleration achieved in one Intel Xeon Phi accelerator. We attained 92 % efficiency with the usage of 64x Intel Xeon Phi accelerators.

### 3. Numerical experiment

We will simulate the collision of two galaxies as a demonstration of our code with mass  $M = 10^{13}M_{\odot}$  and velocity  $v_{cr} = 800\text{km/s}$ . The first galaxy is set by self-gravitating the spherical clouds for the description of gas and collisionless components with an initial distribution of density equilibrium. The star component of the second galaxy has a spiral form. The galaxies are rotating in opposite directions with differential rotation:

$$v_{\phi} = \sqrt{r \frac{\partial \Phi}{\partial r}}.$$

For numerical simulation, a  $512^3$  computational mesh was used. This scenario of galaxy collision used the same NGC 2936/2937 interacting galaxy scenario. The figures show the results of the column density distribution of gas and star components. After the process of collision behind the front of a shock wave, there is an active increase in star formation speed, and molecular hydrogen is formed in future galaxy zones. It should be noted that the growth of the formation is observed in an area that corresponds with the spiral form.

### Conclusion

In paper the new hydrodynamic model of the interacting galaxies is proposed. This model is based on the joint solution of the multicomponent gas dynamics equations, the first moments of the collisionless Boltzmann equation and Poisson's equation for gravity potential. Using of this model gave us possibility to formulate a uniform numerical method of the hyperbolic equations solution. This numerical method is effectively realized for hybrid supercomputers equipped with Intel Xeon Phi accelerators. Computational experiments were performed at the RSC PetaStream architecture cluster of JSCC RAS with 134x acceleration achieved in one Intel Xeon Phi accelerator. We attained 92 % efficiency with the usage of 64x Intel Xeon Phi accelerators. The collision problem of disk and spiral galaxies with increased star formation rate area is simulated.

### Acknowledgments

This work was partially supported by Russian Foundation for Basic Research (grants 15-31-20150, 15-01-00508, and 16-07-00434) and by Grant of the President of Russian Federation for the support of young scientists number MK – 6648.2015.9. This project was partially supported by the Russian Ministry of Education and Science.

### References

- [1] Tutukov A., Lazareva G., Kulikov I. Gas Dynamics of a Central Collision of Two Galaxies: Merger, Disruption, Passage, and the Formation of a New Galaxy // Astronomy Reports. – 2011. – V. 55, I. 9. – P. 770-783.

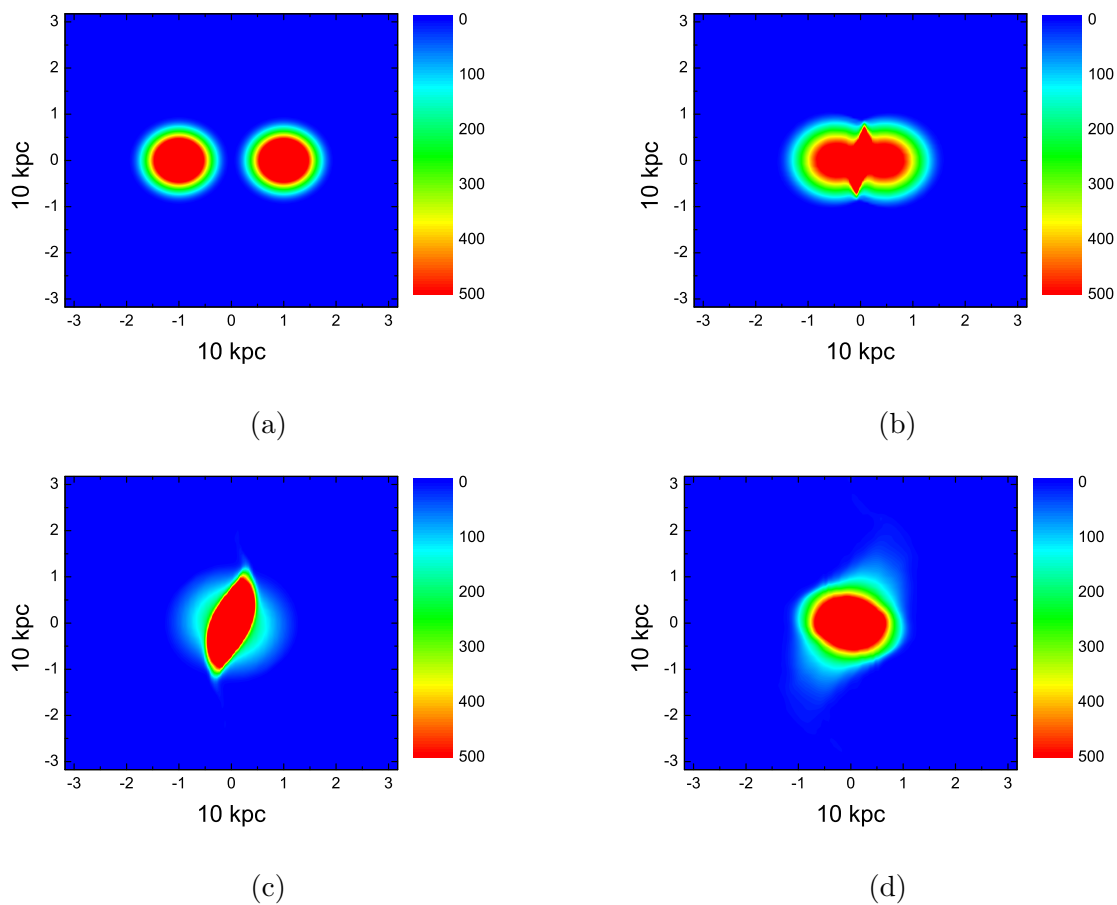


**Figure 1.** Column density in  $M_{\odot}pc^{-2}$  of gas components in time moments  $t = 0$  myr – (a),  $t = 100$  myr – (b),  $t = 200$  myr – (c),  $t = 400$  myr – (d).

- [2] Schweizer F. Merger-Induced Starbursts // Astrophysics and Space Science Library. – 2005. – V. 329. – P. 143-152.
- [3] Sol Alonso M., Lambas D., Tissera P., Coldwell G. Active galactic nuclei and galaxy interactions // Monthly Notices of the Royal Astronomical Society. – 2007. – V. 375, I. 3. – P. 1017-1024.
- [4] Blecha L., Loeb A., Narayan R. Double-peaked narrow-line signatures of dual supermassive black holes in galaxy merger simulations // Monthly Notices of the Royal Astronomical Society. – 2013. – V. 429, I. 3. – P. 2594-2616.
- [5] Rodriguez C., Taylor G., Zavala R., Pihlstrom Y., Peck A. Hi observations of the supermassive binary black hole system in 0402+379 // The Astrophysical Journal. – 2009. – V. 697, I. 1. – P. 37-44.
- [6] Combes F., Melchior A. Chemodynamical evolution of interacting galaxies // Astrophysics and Space Science. – 2002. – V. 281, I. 1-2. – P. 383-387.
- [7] Chilingarian I., Di Matteo P., Combes F., Melchior A., Semelin B. The GalMer database: galaxy mergers in the virtual observatory // Astronomy & Astrophysics. – 2010. – V. 518, A61. – P. 1-14.
- [8] Mitchell N., Vorobyov E., Hensler G. Collisionless Stellar Hydrodynamics as an Efficient Alternative to N-body Methods // Monthly Notices of the Royal Astronomical Society. – 2013. – V. 428. – P. 2674-2687.
- [9] Kulikov I. GPUPEGAS: A New GPU-accelerated Hydrodynamic Code for Numerical Simulations of Interacting Galaxies // The Astrophysical Journal Supplements Series. – 2014. – V. 214, I. 12. – P. 1-12.
- [10] Pearcea F.R., Couchman H.M.P. Hydra: a parallel adaptive grid code // New Astronomy. – 1997. – V. 2. – P. 411-427.
- [11] Wadsley J.W., Stadel J., Quinn T. Gasoline: a flexible, parallel implementation of TreeSPH // New Astronomy. – 2004. – V. 9. – P. 137-158.

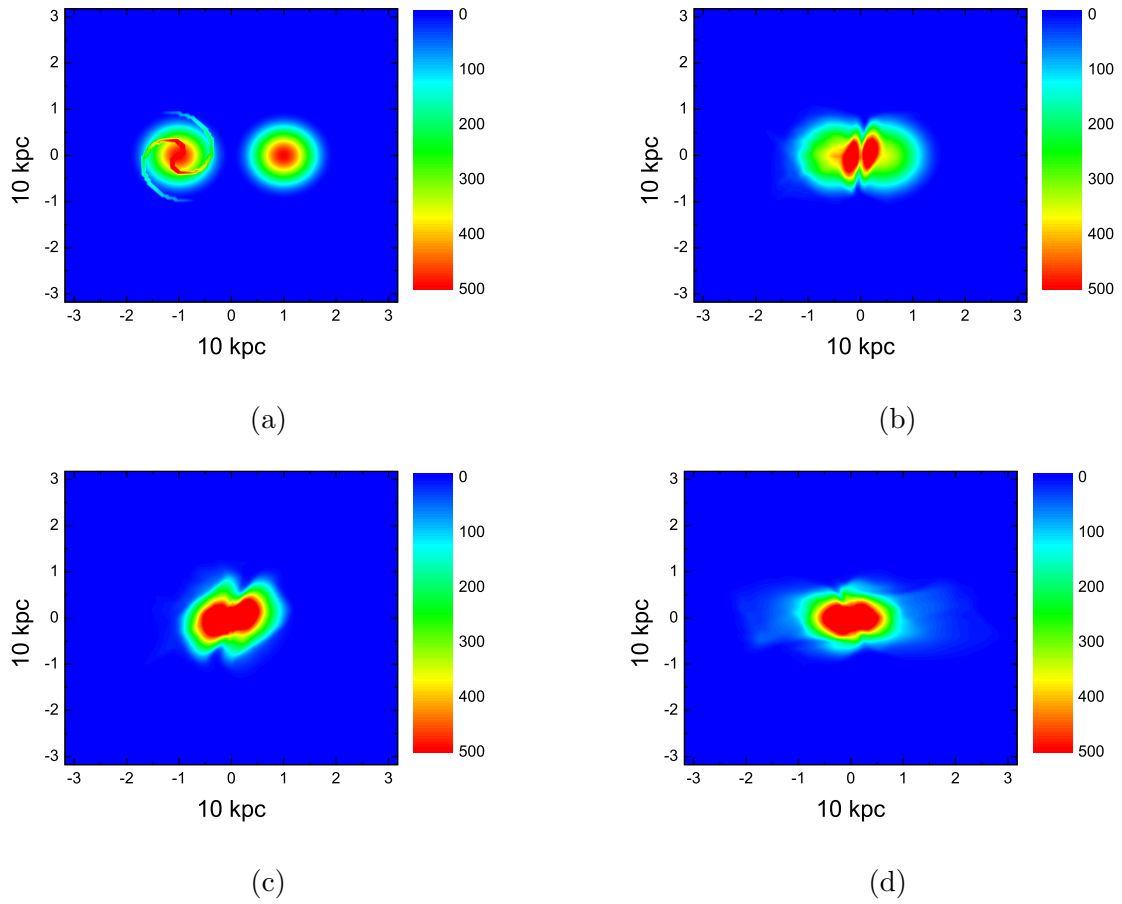


**Figure 2.** Column density in  $M_{\odot}pc^{-2}$  of star components in time moments  $t = 0$  myr – (a),  $t = 100$  myr – (b),  $t = 200$  myr – (c),  $t = 400$  myr – (d).

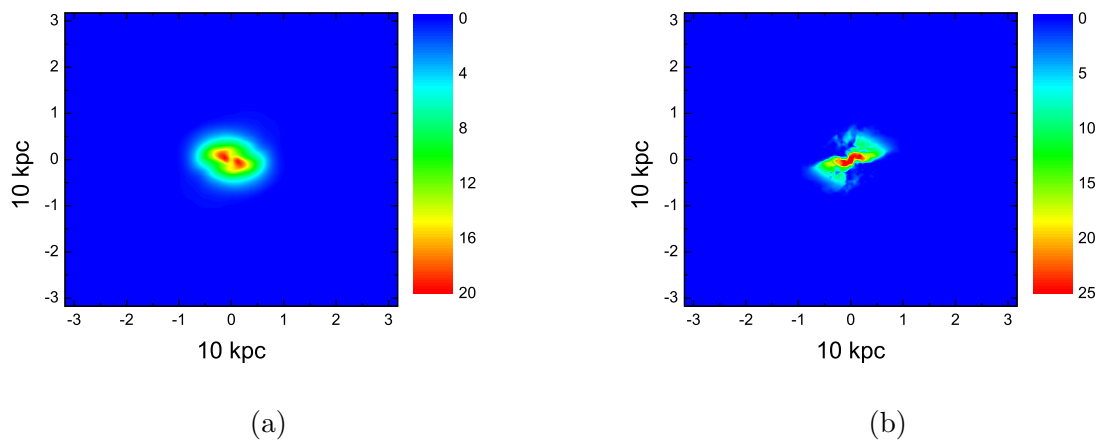


**Figure 3.** Column density in  $M_{\odot}pc^{-2}$  of gas components in time moment  $t = 400$  myr – (a). The rate of star formation process  $M_{\odot}pc^{-2}myr^{-1}$  at time moment  $t = 400$  myr – (b).

[12] Matthias S. GRAPESPH: cosmological smoothed particle hydrodynamics simulations with the special-purpose hardware GRAPE // Monthly Notices of the Royal Astronomical Society. – 1996. – V. 278.



- P. 1005-1017.
- [13] Springel V. The cosmological simulation code GADGET-2 // *Monthly Notices of the Royal Astronomical Society*. – 2005. – V. 364. – P. 1105-1134.
- [14] Ziegler U. Self-gravitational adaptive mesh magnetohydrodynamics with the NIRVANA code // *Astronomy & Astrophysics*. – 2005. – V. 435. – P. 385-395.
- [15] Mignone A., Plewa T., Bodo G. The Piecewise Parabolic Method for Multidimensional Relativistic Fluid Dynamics // *The Astrophysical Journal*. – 2005. – V. 160. – P. 199-219.
- [16] Hayes J., Norman M., Fiedler R. et al. Simulating Radiating and Magnetized Flows in Multiple Dimensions with ZEUS-MP // *The Astrophysical Journal Supplement Series*. – 2006. – V. 165. – P. 188-228.
- [17] O'Shea B., Bryan G., Bordner J., Norman M., Abel T., Harkness R., Kritsuk A. Adaptive Mesh Refinement - Theory and Applications // *Lectures Notes of Computer Science Engineering*. – 2005. – V. 41. – P. 341-350.
- [18] Teyssier R. Cosmological hydrodynamics with adaptive mesh refinement. A new high resolution code called RAMSES // *Astronomy & Astrophysics*. – 2002. – V. 385. – P. 337-364.
- [19] Kravtsov A., Klypin A., Hoffman Y. Constrained Simulations of the Real Universe. II. Observational Signatures of Intergalactic Gas in the Local Supercluster Region // *The Astrophysical Journal*. – 2002. – V. 571. – P. 563-575.
- [20] Stone J. et al. Athena: A New Code for Astrophysical MHD // *The Astrophysical Journal Supplement Series*. – 2008. – V. 178. – P. 137-177.
- [21] Brandenburg A., Dobler W. Hydromagnetic turbulence in computer simulations // *Computer Physics Communications*. – 2002. – V. 147. – P. 471-475.
- [22] Gonzalez M., Audit E., Huynh P. HERACLES: a three-dimensional radiation hydrodynamics code // *Astronomy & Astrophysics*. – 2007. – V. 464. – P. 429-435.
- [23] Krumholz M.R., Klein R.I., McKee C.F., Bolstad, J. Equations and Algorithms for Mixed-frame Flux-limited Diffusion Radiation Hydrodynamics // *The Astrophysical Journal*. – 2007. – V. 667. – P. 626-643.
- [24] Mignone A. et al. PLUTO: a Numerical Code for Computational Astrophysics // *The Astrophysical Journal Supplement Series*. – 2007. – V. 170. – P. 228-242.
- [25] Almgren A. et al. CASTRO: A New Compressible Astrophysical Solver. I. Hydrodynamics and Self-gravity // *The Astrophysical Journal*. – 2010. – V. 715. – P. 1221-1238.
- [26] Schive H., Tsai Y., Chiueh T. GAMER: a GPU-accelerated Adaptive-Mesh-Refinement Code for Astrophysics // *The Astrophysical Journal*. – 2010. – V. 186. – P. 457-484.
- [27] Murphy J., Burrows A. BETHE-Hydro: An Arbitrary Lagrangian-Eulerian Multidimensional Hydrodynamics Code for Astrophysical Simulations // *The Astrophysical Journal Supplement Series*. – 2008. – V. 179. – P. 209-241.
- [28] Springel V. E pur si muove: Galilean-invariant cosmological hydrodynamical simulations on a moving mesh // *Monthly Notices of the Royal Astronomical Society*. – 2010. – V. 401. – P. 791-851.
- [29] Bruenn S. et al. 2D and 3D core-collapse supernovae simulation results obtained with the CHIMERA code // *Journal of Physics*. – 2009. – V. 180. – P. 1-5.
- [30] Hopkins P. A new class of accurate, mesh-free hydrodynamic simulation methods // *Monthly Notices of the Royal Astronomical Society*. – 2015. – V. 450, I. 1. – P. 53-110.
- [31] Vshivkov V., Lazareva G., Snytnikov A., Kulikov I., Tutukov A. Hydrodynamical code for numerical simulation of the gas components of colliding galaxies // *The Astrophysical Journal Supplement Series*. – 2011. – V. 194, I. 47. – P. 1-12.
- [32] Kulikov I.M., Chernykh I.G., Snytnikov A.V., Glinskiy B.M., Tutukov A.V. AstroPhi: A code for complex simulation of dynamics of astrophysical objects using hybrid supercomputers // *Computer Physics Communications*. – 2015. – V. 186. P. 71-80.
- [33] Bergin E., Hartmann L., Raymond J., Ballesteros-Paredes J. Molecular Cloud Formation behind Shock Waves // *The Astrophysical Journal*. – 2004. – V. 612. – P. 921-939.
- [34] Tielens A., Hollenbach D. Photodissociation regions. I - Basic model. II - A model for the Orion photodissociation region // *The Astrophysical Journal*. – 1985. – V. 291. – P. 722-754.
- [35] Cazaux S., Tielens A.  $H_2$  Formation on Grain Surfaces // *The Astrophysical Journal*. – 2004. – V. 604. – P. 222-237.
- [36] Caselli P., Walmsley C., Terzieva R., Herbst E. The Ionization Fraction in Dense Cloud Cores // *The Astrophysical Journal*. – 1998. – V. 499. – P. 234-249.
- [37] Bergin E., Plume R., Williams J., Myers P. The Ionization Fraction in Dense Molecular Gas. II. Massive Cores // *The Astrophysical Journal*. – 1999. – V. 512. – P. 724-739.
- [38] Van Der Tak F., Van Dishoeck E. Limits on the cosmic-ray ionization rate toward massive young stars // *Astronomy & Astrophysics*. – 2000. – V. 358. – P. L79-L82.
- [39] Draine B., Bertoldi F. Structure of Stationary Photodissociation Fronts // *The Astrophysical Journal*. –

1996. – V. 468. – P. 269-289.
- [40] Draine B. Photoelectric heating of interstellar gas // The Astrophysical Journal Supplement Series. – 1978. – V. 36. – P. 595-619.
- [41] Glover S., Mac Low M. Simulating the Formation of Molecular Clouds. I. Slow Formation by Gravitational Collapse from Static Initial Conditions // The Astrophysical Journal Supplement Series. – 2007. – V. 169, I. 2. – P. 239-268.
- [42] Katz N., Weinberg D., Hernquist L. Cosmological simulations with TreeSPH // The Astrophysical Journal Supplement Series. – 1996. – V. 105. – P. 19-35.
- [43] Springel V., Hernquist L. Cosmological smoothed particle hydrodynamics simulations: a hybrid multiphase model for star formation // Monthly Notices of the Royal Astronomical Society. – 2003. – V. 339, I. 2. – P. 289-311.
- [44] Sutherland R., Dopita M. Cooling functions for low-density astrophysical plasmas // The Astrophysical Journal Supplement Series. – 1993. – V. 88. – P. 253-327.
- [45] Popov M., Ustyugov S. Piecewise parabolic method on local stencil for gasdynamic simulations // Computational Mathematics and Mathematical Physics. – 2007. – V. 47, I. 12. – P. 1970-1989.
- [46] Popov M., Ustyugov S. Piecewise parabolic method on a local stencil for ideal magnetohydrodynamics // Computational Mathematics and Mathematical Physics. – 2008. – V. 48, I. 3. – P. 477-499.
- [47] Roe P. Approximate Riemann solvers, parameter vectors, and difference solvers // Journal of Computational Physics. – 1997. – V. 135. – P. 250-258.
- [48] Collela P., Woodward P.R. The Piecewise Parabolic Method (PPM) Gas-Dynamical simulations // Journal of Computational Physics. – 1984. – V. 54. – P. 174-201.
- [49] Kulikov I., Vorobyov E. Using the PPML approach for constructing a low-dissipation, operator-splitting scheme for numerical simulations of hydrodynamic flows // Journal of Computational Physics. – 2016. (submitted)
- [50] Vshivkov V., Lazareva G., Snytnikov A., Kulikov I., Tutukov A. Computational methods for ill-posed problems of gravitational gasodynamics // Journal of Inverse and Ill-posed Problems. – 2011. – V. 19, I. 1. – P. 151-166.
- [51] Godunov S., Kulikov I. Computation of Discontinuous Solutions of Fluid Dynamics Equations with Entropy Nondecrease Guarantee // Computational Mathematics and Mathematical Physics. – 2014. – V. 54, I. 6. – P. 1012-1024.